IEEE Access
Multidisciplinary | Rapid Review | Open Access Journal

Received August 31, 2021, accepted September 14, 2021, date of publication September 16, 2021,
date of current version September 24, 2021.

Digital Object Identifier 10.1109/ACCESS.2021.3113332

Investigation on Impact of Magnetic Field on the Corona Discharge Activity in Punga Oil Using Fluorescent Fiber and UHF Sensor Techniques

SRINIVASAN MURUGESAN[1], (Member, IEEE), A. J. AMALANATHAN[2], R. SARATHI[2], (Senior Member, IEEE), BALAJI SRINIVASAN[2], (Member, IEEE), AND RAVI SAMIKANNU[3], (Senior Member, IEEE)

[1]Department of Electrical and Electronics Engineering, Kongu Engineering College, Erode 638060, India
[2]Department of Electrical Engineering, Indian Institute of Technology Madras, Chennai 600036, India
[3]Department of Electrical, Computer and Telecommunications Engineering, Botswana International University of Science and Technology, Palapye, Botswana

Corresponding author: Srinivasan Murugesan (msrinieee@gmail.com)

This work was supported in part by the Department of Electrical Engineering, Indian Institute of Technology Madras, Chennai, through the Science and Engineering Research Board (SERB) Teachers Associateship for Research Excellence Scheme, under Grant TAR/2020/000149.

ABSTRACT This paper reports the experimental investigation of the corona discharge activity of punga oil under the influence of a local magnetic field and different voltage profiles (AC and DC voltages) using fluorescent fiber sensor as well as UHF sensor technique. The corona inception voltage (CIV) of punga oil is higher under negative DC voltage followed by positive DC and AC voltage, with a marginal reduction in its CIV magnitude observed on the impact of external magnetic field. The dominant frequency of the UHF signal obtained under AC voltage shifted towards lower frequency (0.6 GHz) with the influence of magnetic flux density to about 85 mT. The rise time, pulse width and energy content of the fluorescent signal formed due to corona activity under AC voltage is found to vary under high magnetic fields confirming the inception results. The fluorescent signals formed due to corona discharge under both AC and DC voltages have its dominant frequency at 1 MHz with no shift observed in the presence of magnetic field. Also, there is no variation in the phase resolved partial discharge (PRPD) pattern observed due to corona discharge (with and without magnetic field) signal using both UHF sensor and the fluorescent sensor. The fluorescent fiber-based technique provides a better accuracy on detecting the corona discharges in punga oil at an early stage compared to conventional UHF sensor. The breakdown voltage of punga oil under different voltage profiles with and without the effect of magnetic field follows normal distribution. The dielectric dissipation factor and electrostatic charging tendency (ECT) of punga oil is observed to be higher than the limit set for insulating fluids towards power transformer operation.

INDEX TERMS Corona discharge, magnetic field, fluorescent fiber, UHF sensor, rise time, streaming current.

I. INTRODUCTION

The insulation design of oil-filled power transformers is vital for their longevity and reliable operation in a power system network. Mineral oils have been traditionally used as an insulant and coolant in the power transformers. However, with the recent shortfall of the global oil supply and a general depletion of non-renewable sources, a serious shortage may be expected in the near future [1]. While installing the transformers, fire protection is a primary concern, as they are frequently positioned in high-risk situations such as within buildings and underground installations. Nevertheless, the higher thermal class of ester fluids [2] compared to mineral oil makes them suitable to be placed closer to the buildings, resulting in lower power losses. In view of this, alternative insulants such as vegetable oils (soybean, sunflower, punga) are now being tested for transformer applications [3]. In comparison to the conventional mineral oil, these ester-based fluids derived from various plant seeds have shown better fire class properties with increased

The associate editor coordinating the review of this manuscript and approving it for publication was Mira Naftaly.

biodegradability [4], [5]. Punga oil (non-edible) have been used nowadays for transformer applications [6]. In the present work, punga oil has been considered to understand its performance in partial discharge behaviour and dielectric properties. Punga oil derived from Milletia pinnata tree has a variety of fatty acids (oleic, palmitic and stearic) that determines the physico-chemical and dielectric properties of the insulating oil [7]. Mariprasath *et al.* [8] have studied the dissolved gas analysis (DGA) on both punga oil and mineral oil, inferring a lower combustible gas in the former compared to the latter. In addition, the breakdown strength of punga oil is higher than conventional mineral oil along with a low moisture content inferred at higher ageing duration [9], [10]. The permittivity of punga oil and cellulosic paper/pressboard insulation are in the same range [11] and thus causing the localized electric field to be much lesser in punga oil impregnated pressboard material compared to mineral oil.

One of the most common reasons for transformer insulation failure is corona discharge caused by protrusion [11] from the winding conductor or at the ground electrode. Identification of such incipient discharges formed due to corona activity is difficult, and numerous approaches are employed (phase acoustic emission technique, radio frequency (RF) methodology, dissolved gas analysis) to detect them at an early stage [12]. The injected current pulses arising due to the partial discharges in transformers is found to be in the range of nanoseconds [13], thereby exciting electromagnetic signals in the range of 0.3-3 GHz (Ultra high frequency (UHF) region). As such, various literature has been published on the use of the UHF approach [14] for the detection of partial discharges (PD). On the other hand, fluorescent fiber sensor is another interesting technique for PD detection but the choice of a suitable fluorescent fiber for detecting PD activity depending on the physical properties of insulating fluid and its comparison with the UHF technique has not been reported. Another interesting aspect of PD detection is the dependence on the external magnetic field. According to the classical electromagnetic theory, the impact of external magnetic field in addition to applied electric field can alter the PD behaviour and hence it is necessary to understand the effect of magnetic field subjected to both AC and DC electric fields. The leakage flux densities involved in the power transformers varies from 60 mT-700 mT [15] and in the present work, the lower range of magnetic fields are experimented for its performance towards the punga oil. Martinez-Tarifa *et al.* [15] has simulated the magnetic flux estimation in power transformers using finite element method (FEM) and concluded that direction of magnetic flux may adopt different patterns with not much variation in the magnitude of flux density. Thus, constant magnetic field has been considered in the present research work for understanding PD activity in punga oil. With the effect of magnetic field involved in the system, the conventional UHF technique of PD detection can mislead on the classification discharges and hence, the fluorescent fiber-based technique has been used for its comparison over the conventional UHF sensor. Along with the above studies on PD detection, it is also essential to investigate the phase resolved partial discharge (PRPD) pattern under the effect of both electric and magnetic field with a statistical distribution on the breakdown voltage exhibited by the punga oil. An interesting aspect of fluorescent fiber-based sensing is that the vegetable oils are rich in vitamin E and unsaturated fatty acids that are fluorescent in nature, and its characteristics gets altered depending on the chemical structure of ester fluids [16]. The fluorescence spectroscopic measurements of insulating fluids should be performed pre-requisite to its installation inside the transformers, which enables proper selection of fluorescent fiber, for identification of incipient discharges in transformer insulation. Static electrification is another major phenomenon occurring in the oil filled transformers, where the insulating fluid used for heat transfer causes a charge separation at the paper/pressboard interface, forming an electrical double layer [17]. These charged ions over a longer time interval can lead to complete flashover of the pressboard spacers. There are different techniques employed for the detection of charging current at the oil/pressboard interface and in the present work, the spinning disc system [18] has been employed to investigate the electrostatic charging tendency (ECT) of punga oil because of its lesser requirement on the oil volume and pre-processing time.

In line with the above discussion, the following experimental studies have been carried out with punga oil in this work: (i) Fluorescence optical fiber sensor and UHF sensor techniques were adopted to identify the variation in corona inception voltage with and without magnetic field, under AC and DC voltages (ii) Parametric evaluation of PD based on UHF and fluorescent fiber generated signal, (iii) Statistical analysis on the breakdown strength of punga oil with and without magnetic field, (iv) Variation in the permittivity and loss tangent of punga oil at different frequencies and (v) Electrostatic charging tendency of punga oil with the pressboard material at different temperatures.

II. EXPERIMENTAL DETAILS

A. HIGH VOLTAGE SOURCE AND SENSOR

Fig. 1 shows the experimental setup for measuring the corona inception voltage. The desired range of high voltage for this experiment is generated by a Trek amplifier (Model 20/20C) with an appropriate input from a function generator. For the breakdown investigations, a 100 kV, 5 kVA, 50 Hz transformer was utilized to generate the AC voltage, while a voltage doubler circuit was employed to generate the DC voltages. During the breakdown measurements on the punga oil, the voltage was increased at a constant rate of 300 V/s. For every 5 breakdowns, the needle electrode was replaced during experimental studies to avoid variation in breakdown voltage due to change in the conductivity occurring at the needle tip. After every breakdown, it was also ensured that the gap between the needle electrode and the ground is free from any carbon track or bubbles formed due to previous

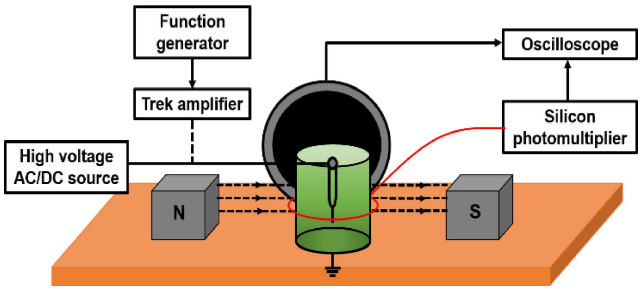

FIGURE 1. Experimental setup for corona inception studies on punga oil.

breakdown. To simulate the corona discharge activity in punga oil, the needle-plane electrode configuration is used in the present study. The needle electrode with radius of curvature about 50 μm is used. As per the CIGRE references [19], the electrode size or the needle tip radius for liquid insulation studies can range from 3 to 100 μm with the ground electrode diameter is 50 mm. The gap distance between the needle and ground was maintained as 5 mm to investigate the performance of corona discharges for lower gap spacing's and further it can also be compared with the previous research by the authors [16], [20] where similar configuration was used for experiments.

A uniform magnetic field is applied in addition to the electric field, and its flux density is varied by placing the magnet at different locations with symmetric gap spacing away from the test cell. A Digital gauss meter (DGM-202) with a Hall probe was used to calibrate the magnetic field magnitude |B| at the needle tip and the background magnetic fields were taken into account when calibrating the field probe. The experiments were performed in a completed dark room similar to the case inside the power transformers for better validation on fluorescence fiber results. In the case of UHF sensor, the trigger level maintained was higher than noise level for its higher accuracy. The UHF signal generated based on rate of rise of injected current and it is well known that based on the rate of rise of injected corona /surface discharge activity, the rate of rise of current formed lies in nano second range and in frequency bandwidth lies in the UHF range [13]. In the case of fluorescent fiber technique, the signal output depends on the duration of the light emission during the discharge process [21]. The fluorescent fiber sensor technique for corona detection is implemented using a 1 m long and 1 mm diameter red as well as white fluorescent fiber (Saint Gobain Crystals BCF 91A) and a silicon photomultiplier (SiPM, SensL MicroFC SMA 10050) module. The fluorescent fiber's emission properties and responsivity of silicon photomultiplier (SiPM) sensor overlap, indicating that the fluorescent fiber and the SiPM detector are compatible for PD detection. The bandwidth of the fluorescence sensor depends on various factors such as bias voltage, positioning of fiber and light source intensity. SiPM can easily detect low light signals with rise times as rapid as a few nanoseconds, according to its specifications [22]. Due to the relatively higher fluorescence life times, quick light emissions are measured by the photo detector and transformed to voltage signals with fast rise times and extended fall times. To enhance the output signal to the necessary voltage range, voltage amplifier is usually employed where it improves the measurement with its bandwidth restricted to 1300 MHz. The fibre is looped around the test cell with one end pointing towards the needle tip and other end is inserted into the SiPM module, which is biased at 30 V. The unexposed region of the fiber is covered with an opaque sleeve to prevent background radiation. Simultaneous measurements are performed using a non-directional broadband UHF sensor (3 GHz bandwidth) placed at 20 cm away from the test cell for its higher sensitivity [13]. Signals from both the UHF sensor and fluorescent fiber sensor used for detecting the corona discharge activity are then fed into a digital storage oscilloscope (3.5 GHz bandwidth, 40 GSa/s) with an input impedance of 50 Ω.

B. DIELECTRIC RESPONSE AND FLUX DENSITY MEASUREMENT

The measurement of the dielectric response of the punga oil is carried out by generating sinusoidal signals at different frequencies using OMICRON-DIRANA instrument as shown in Fig. 2. The oil test cell is connected to a DIRANA dielectric response analyzer using three electrodes: voltage, measurement, and guard electrodes, as per the IEC 60247 standard [23]. The normal operating temperature of oil immersed transformer is around 65°C and sometimes due to the localised hotspot formation, the temperature can go upto 90°C as per IEC 60076-2 standard [24]. Thermal equilibrium condition is maintained during the measurement time interval as the samples are heated from 30°C to 90°C using a heating system that allowed a maximum temperature of around 110°C.

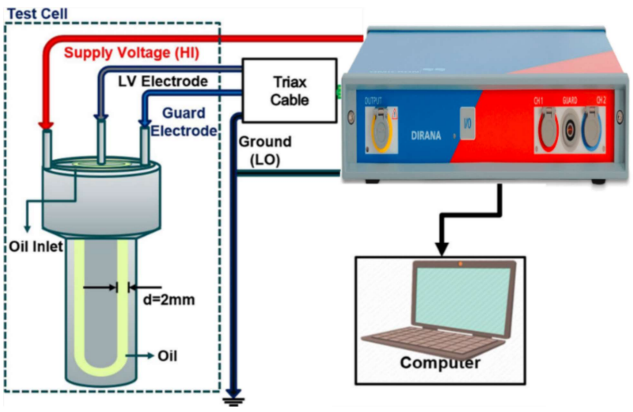

FIGURE 2. Schematic diagram of experimental setup used for dielectric response measurements.

C. FLOW ELECTRIFICATION

A spinning disc equipment was employed to measure the streaming current, with the cellulose material covering both sides of the disc as indicated in Fig. 3. An aluminium disc (40 mm dia × 6 mm thick) was employed in the present work as per CIGRE references [25]. The cylindrical vessel

housing the insulating fluid was also made of aluminium (85 mm dia × 100 mm ht.), where the centrifugal force governing the separation of charges at the oil/pressboard interface were convected towards the walls of vessel and then measured using a Keithley electrometer (6517B). The spinning of the disc is controlled in the range 0 to 600 rpm using motor coupled with a speed regulator. While performing the measurements with the effect of the temperature, a digital thermometer is used within the oil matrix to continuously monitor the change in the temperature equilibrium. To limit the intrusion of stray current from affecting the actual measurements, both the spinning disc system and the motor were enclosed inside the Faraday cage.

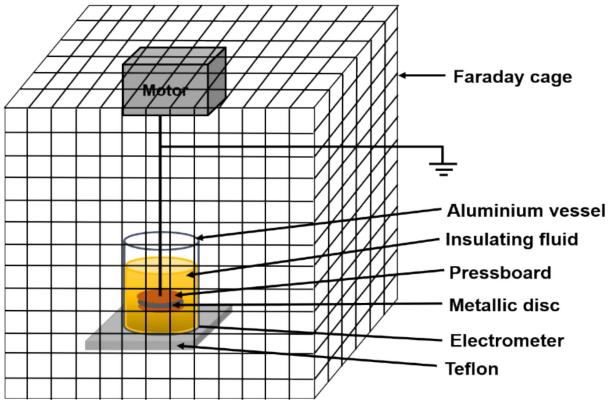

FIGURE 3. Spinning disc system used for flow electrification studies.

III. RESULTS AND DISCUSSIONS

A. STEADY STATE EXCITATION EMISSION MATRIX OF PUNGA OIL

A Horiba aqualog spectrofluorometer with a 150 W xenon lamp is used to measure the fluorescence spectra of punga oil. Fig. 4 shows the excitation-emission matrix (EEM) of punga oil obtained with excitation wavelength from 350 to 650 nm at an interval of 15 nm and emission wavelength from 300 to 1000 nm at an interval of 1.1 nm. The colour scale graph indicated in Fig. 4 represents the emission intensity of fluorophore (punga oil). The unsaturated fatty acids and chemical structure of punga oil [26] acts as a primary source of fluorescence behaviour, where its emission and excitation wavelength are observed in the range of 500-850 nm and 500-650 nm.

The fluorescent fiber used for corona discharge studies of punga oil must contain its absorption and emission peak confining to these spectral wavelengths. The excitation spectrum of fluorescent substances should be within the range of the created PD spectrum to ensure that the produced PD light signal is detected by the fluorescent fiber. A wide range of plastic scintillating, wavelength-shifting, and light-transmitting fibres [27] are used nowadays in various research applications. The red and white fiber belongs to wavelength shifting fibers possessing a larger Stokes shift cascading photons from near UV to blue, followed by green and then yellow or red

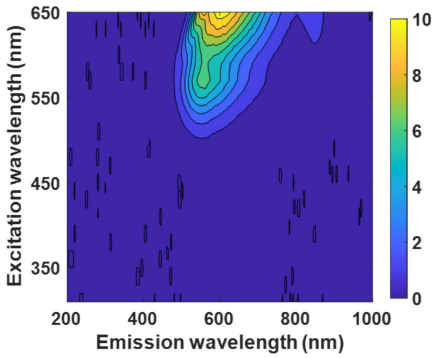

FIGURE 4. EEM spectra of punga oil.

wavelengths [28]. The application of different fibers tested towards PD detection in transformers [29] and in the present work, the red and white fiber was chosen since its excitation and emission characteristics are similar to that of punga oil. Similar studies can also be performed for mineral oil, where its fluorescence characteristics are nearer to 350-400 nm [30] suggesting the usage of green fiber rather than red and white fiber used for punga oil. One of the objectives of the present study is to identify a suitable fluorescent fiber (Table 1), which need to be chosen for its better performance towards corona detection. This indicates that a suitable fluorescent fiber has to be chosen for its better performance towards corona detection. Since the fluorescence behaviour of punga oil and mineral oil are different with respect to its excitation and emission wavelength, the fluorescent fiber used also gets varied for different insulating oils. Thus, on understanding the EEM spectra of fluid, the type of fluorescent fiber suitable for detecting corona discharges could be selected and this steady state fluorescence spectroscopy can also be used as a condition monitoring technique for assessing the quality of the insulating fluid.

TABLE 1. Emission and absorption spectral characteristics of fluorescent fiber.

Description of fluorescent fiber	Emission spectral peak (nm)	Absorption spectral peak (nm)
Y-8 (100)	511	455
R-3 (100)	610	577
Y-11 (200)	476	430
B-3 (200)	450	351

B. CORONA DISCHARGE USING FLUORESCENT FIBER AND UHF SENSOR

The corona inception voltage (CIV) of punga oil is determined by UHF and fluorescent fibers (red fiber, white fiber) under both AC and DC voltages. The first discharge pulse detected by the oscilloscope from the UHF sensor output and optical emission in the case of fluorescent fiber was considered as CIV in the present investigation.The reported values are based on average of 30 observations, and the first

discharge recorded by the UHF sensor and fluorescent fibre was chosen as CIV. The measured values were determined to have a standard deviation of less than 3% and hence not indicated Fig. 5.

1) WITHOUT MAGNETIC FIELD

The CIV of punga oil measured in the absence of magnetic field is shown in Table 2. Higher CIV values are observed under negative DC voltage followed by positive DC and AC voltage. The electric field exerted at the needle electrode (high voltage) aids the applied electric field under positive polarity, thereby initiating discharges to occur at lower voltages compared to negative polarity. In case of AC voltage, the space charge injected from the needle tip in the negative half cycle impacts the electric field formed during the positive half cycle [11] and thus cause lower CIV compared to DC voltages. On comparing the efficiency of both UHF and fluorescence fibers, the white fiber has shown early detection of CIV compared to red fiber and UHF sensor. This is because of higher sensitivity of fluorescent fiber sensors to corona discharges compared to UHF sensor [22] and proper selection of fiber based on the characteristics of the fluid.

TABLE 2. CIV of punga oil without magnetic field adopting UHF sensor and fluorescent fibers.

Voltage profile	Type of sensor		
	UHF	Red fiber	White fiber
AC	16.08	14.36	13.89
+DC	26.48	24.54	23.76
−DC	28.92	26.85	25.43

2) WITH MAGNETIC FIELD

The CIV of punga oil under the influence of magnetic field of different flux density is shown in Fig. 5. A uniform flux density with different magnitudes were obtained by maintaining a symmetrical gap spacing from the test cell towards both the magnets (Fig. 1). The fluorescent fiber showed a better accuracy on detecting the discharges similar to that observed without magnetic field.

It is observed that when applied magnetic field of about 85 mT exerted towards the fluid, a marginal reduction in the inception voltage to about 40% is observed under AC voltage and its effect was negligible at magnetic field of less than 78 mT. However, the effect of magnetic fields on DC voltages (both +DC and −DC) did not indicate a substantial reduction, with the exception of about 6% reduction in CIV value at a flux density of 85 mT.

3) SIGNAL ANALYSIS

The typical signal patterns of UHF and fluorescence sensor measured during corona discharge activity is shown in Fig. 6. To compare the signals obtained using both UHF and fluorescent fiber sensor, due to corona discharges, the normalization

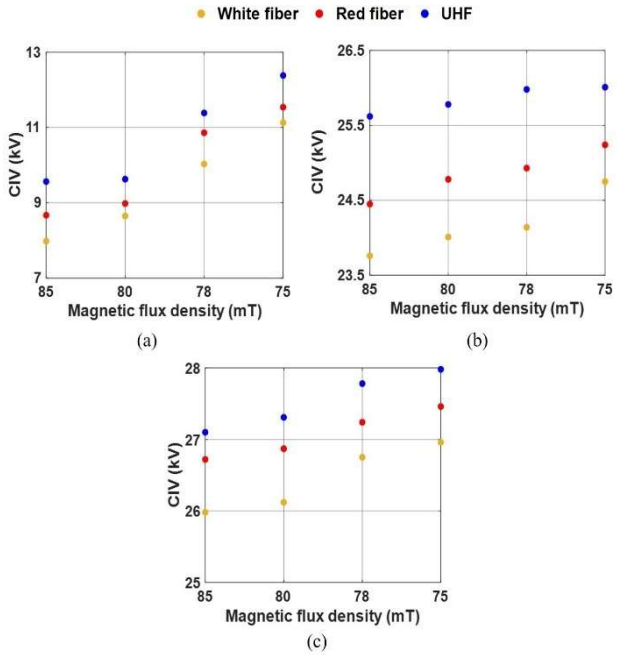

FIGURE 5. CIV of punga oil under the influence of magnetic field for (a) AC voltage, (b) +DC voltage, (c) −DC voltage.

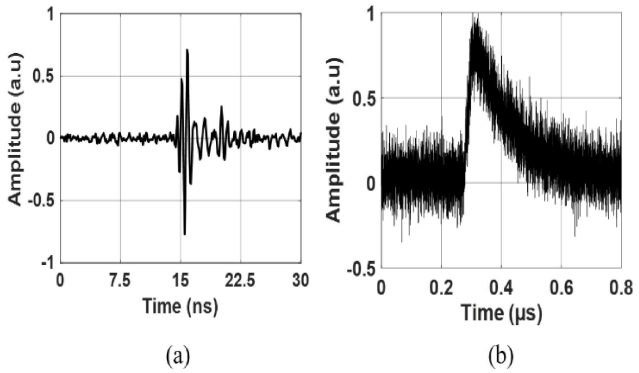

FIGURE 6. Typical signal measured using (a) UHF sensor, (b) fluorescence sensor.

of experimental data was carried out as:

$$Y_i = \max_{1 \le i \le n} \frac{y_i}{|y_i|} \tag{1}$$

where Y_i is the normalized amplitude of voltage at i^{th} point, y_i is the amplitude of the voltage signal at i^{th} point and n indicate the number of sampling points involved in the signal.

Fig. 7 shows the Fast Fourier Transform (FFT) of UHF and fluorescence signal under both AC and DC voltages in the absence of magnetic field. In the case of UHF, frequency content ranges from 300 MHz to 1 GHz, with its dominant frequency observed at 0.9 GHz (Fig. 7a). The fluorescence signal produced at the photomultiplier output was comparable to a double exponent pulse, with an energy content ranging from 0 to 20 MHz and dominant frequency at 1 MHz using both red and white fluorescent fiber (Fig. 7b and Fig. 7c).

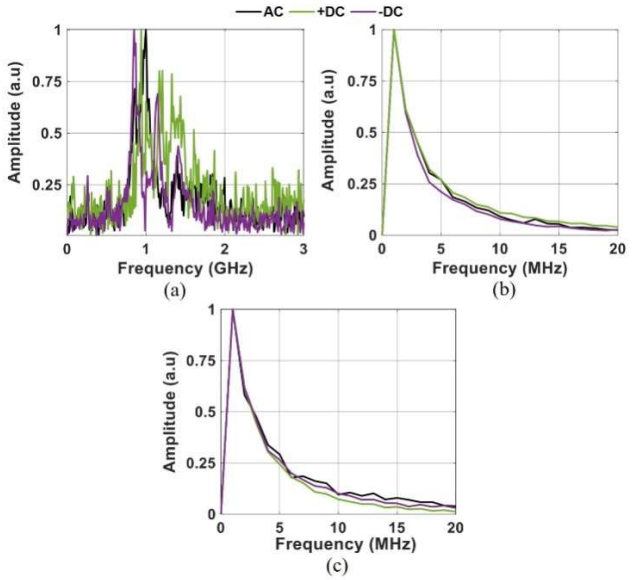

FIGURE 7. Spectrum of the signal without magnetic field using (a) UHF sensor, (b) red fiber, (c) white fiber.

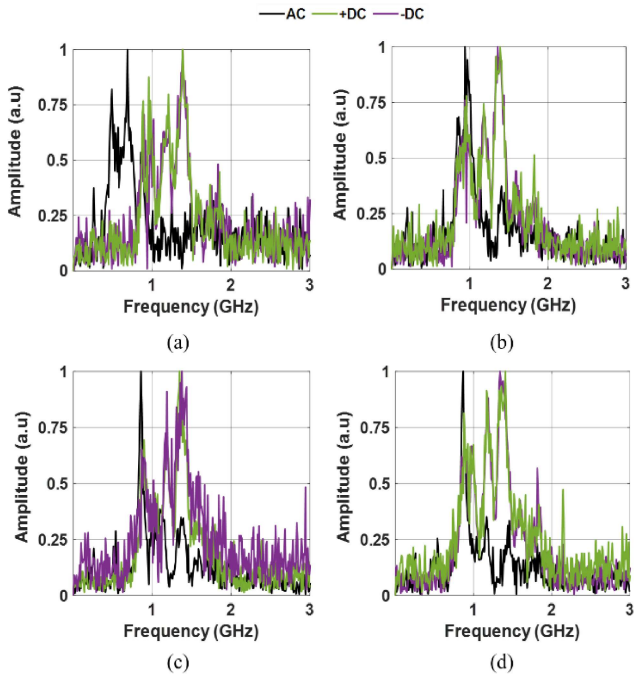

FIGURE 8. FFT of UHF signal with a flux density of (a) 85 mT, (b) 80 mT, (c) 78 mT, (d) 75 mT.

It is also seen that irrespective of the voltage profile, both the bandwidth and dominant frequency of the UHF and fluorescent fiber sensor are in the same range. The frequency spectrum of UHF signal analysis performed with the effect of magnetic field is shown in Fig. 8. On considering the effect of discharges captured under AC voltage, the UHF signal acquired with the effect of magnetic flux density of 85 mT showed a shift in its dominant frequency from around 0.4 to 0.6 GHz (Fig. 8a) compared to its influence without magnetic

TABLE 3. Signal parameters from UHF sensor under both AC and DC voltages.

B_{max}	AC voltage			+DC voltage			−DC voltage		
	t_r (ns)	t_{pw} (ns)	E (fJ)	t_r (ns)	t_{pw} (ns)	E (fJ)	t_r (ns)	t_{pw} (ns)	E (fJ)
0	0.54	1.75	1.5	1.76	1.56	1.9	1.86	1.41	2.1
85	0.87	2.13	2.3	1.83	1.69	2.5	1.90	1.57	2.7
80	0.72	1.64	1.8	1.82	1.53	2.3	1.81	1.52	2.5
78	0.65	1.45	1.6	1.74	1.48	2.1	1.79	1.40	2.2
75	0.51	1.42	1.2	1.69	1.39	1.7	1.73	1.23	1.9

TABLE 4. Signal parameters from redfiber under both AC and DC voltages.

B_{max}	AC voltage			+DC voltage			−DC voltage		
	t_r (µs)	t_{pw} (µs)	E (pJ)	t_r (µs)	t_{pw} (µs)	E (pJ)	t_r (µs)	t_{pw} (µs)	E (pJ)
0	1.36	0.27	0.4	1.89	0.32	1.1	1.84	0.36	1.6
85	1.67	0.46	0.9	1.98	0.47	1.4	1.97	0.45	2.1
80	1.54	0.38	0.8	1.76	0.41	1.3	1.93	0.41	1.9
78	1.48	0.37	0.7	1.63	0.39	1.2	1.86	0.37	1.9
75	1.41	0.32	0.6	1.61	0.34	1.1	1.78	0.36	1.6

field where dominant frequency occurs at 0.9 GHz to 1 GHz (Fig. 7a). At a flux density of less than or equal to 80 mT (Fig. 8b to Fig. 8d), not much change is observed in its spectrum. Although the corona inception voltage under DC voltages did not show much impact in its magnitude with the effect of magnetic field, the signal captured under different flux densities showed a shift from its dominant frequency of 0.9 GHz (Fig. 7a) to 1.35 GHz (Fig. 8a to Fig. 8d).

With the effect of magnetic field, the injected current pulse that initiates the electromagnetic waves during PD activity gets distorted, showing a shift in the UHF frequency spectrum. This change in the UHF signal on the addition of magnetic field can lead to misclassification of discharges during its condition monitoring in power transformer. But the fluorescent fiber technique does not involve any shift in the frequency spectrum even in the presence of magnetic field. Along with the above advantages, the fiber optic-based PD detection provides better resistance towards electromagnetic interference [31] and thus indicating a better accuracy compared to the conventional UHF sensor. The signal recorded with the UHF sensor and fluorescent fiber can be linked to corona discharge activity, with their parameters shown in Table 3 to Table 5 for both AC and DC voltages. The rise time (t_r) is measured from 10% to 90% of the rising peak while the pulse width (t_{pw}) is the elapsed time between the 5% of its rise time and 5% of decay time along with the same limit used for calculation of energy (E) as [32]:

$$E_i = E_{i-1} + \Delta t_s . \sum_{i=0}^{n} \frac{V_i}{R_L} \tag{2}$$

where E_i is the energy of the signal at i^{th} sampling point of signal, V_i denotes the peak-to-peak voltage for UHF signals and due to unipolarity of fluorescent fiber signals,

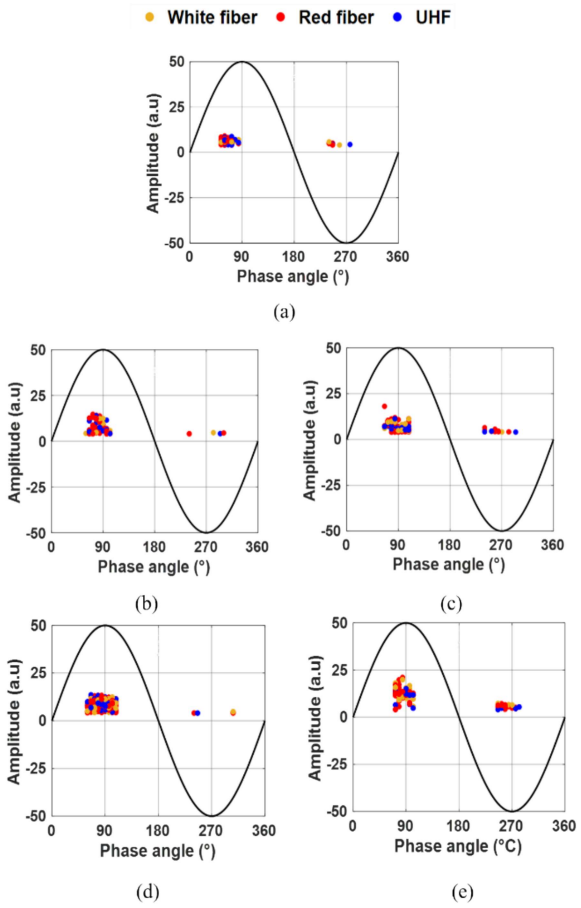

FIGURE 9. PRPD pattern of discharges with (a) no magnetic field, (b) 85 mT, (c) 80 mT, (d) 78 mT, (e) b) 75 mT.

it is considered for only peak voltages, R_L is the measured impedance and Δt_s is the sampling time interval.

The rise time, pulse width and energy content of the fluorescent signal is found to be higher at flux density of 85 mT compared to a flux density of less than 80 mT. The higher distortions involved in the current pulse during the PD activity can result in a burst kind of PD pulses. This change exhibited at the needle tip for higher magnetic fields can increase the intensity of light emitted and thus, the parameters related to the fluorescence signal increases. Also, the effect of DC voltages has shown a higher magnitude of energy compared to AC voltage, indicating its severity towards the corona discharges.

4) PHASE RESOLVED PARTIAL DISCHARGE ANALYSIS

The PRPD analysis of punga oil performed with and without the magnetic field is shown in Fig. 9. To compare the performance of punga oil with and without magnetic field, the voltage was kept at 20% above the CIV and the PRPD signal was monitored to compare the magnitude and phase of the discharges. The spectrum analyzer was connected to the output of UHF sensor and SiPM module for PRPD analysis. Also, the spectrum analyzer was set to zero span mode, with the center frequency matching the same as that of dominant

TABLE 5. Signal parameters from white fiber under both AC and DC voltages.

B_{max}	AC voltage			+DC voltage			−DC voltage		
	t_r (μs)	t_{pw} (μs)	E (pJ)	t_r (μs)	t_{pw} (μs)	E (pJ)	t_r (μs)	t_{pw} (μs)	E (pJ)
0	1.69	0.31	0.5	1.76	0.35	1.5	1.82	0.38	1.8
85	1.83	0.42	0.8	1.87	0.45	1.9	1.87	0.42	2.1
80	1.72	0.40	0.7	1.85	0.43	1.8	1.85	0.41	1.9
78	1.65	0.36	0.6	1.73	0.40	1.6	1.79	0.37	1.8
75	1.53	0.28	0.6	1.72	0.37	1.6	1.67	0.32	1.7

frequency observed from FFT analysis (Fig. 7 and Fig. 8). During the measurement time period, the spectrum analyzer was synchronized with the function generator output, which was utilized to apply high voltage across the test cell using the Trek amplifier. This allows the discharge activity to be correlated with the phase of occurrence of the applied AC voltage. It is observed that most of the discharges have occurred at the maximum phase angle of the supply voltage. Further, the corona discharges were found to be less in the negative half cycle compared to positive half cycle even with the presence of magnetic field. It is concluded that phase occurrence of discharge in punga oil did not show any significant variation with the effect of different magnetic fields.

C. VARIATION IN BREAKDOWN VOLTAGE OF PUNGA OIL WITH MAGNETIC FIELD

Fig. 10 shows the variation in the breakdown voltage of punga oil with the effect of different magnetic flux densities and voltage profiles. The sample's breakdown voltage was calculated using an average of 25 breakdown voltage readings. It is observed that compared to breakdown strength under positive DC and AC voltages, the electrode gap's breakdown strength is higher under negative DC voltage. Under DC voltage, the space charge injected at the needle tip weakens the boundary electric field reducing the streamer propagation [33]. But the alternating waveform involved in AC supply voltage causes ionization of charges at the needle tip during the positive half cycle and in the negative half cycle, the charges formed tries to reduce the gap spacing [11] between the needle tip and ground thereby initiating discharges to occur at a lower voltage compared to its impact under DC voltages. The streamers developed on the negative electrode are highly branched, and their propagation rate is limited due to the lower diffusion of charge carriers, which could have resulted in a more abrupt reduction in the breakdown voltage in both AC and positive DC voltage compared to negative DC voltage.

The breakdown voltage of punga oil under AC voltage with flux density of 85 mT reduced to about 42% compared to its effect without magnetic field and the effect was less observed at a flux density of 75 mT. Unlike the AC voltage profile, the breakdown voltage of punga oil did not show any variation with different magnetic fields exerted along with the application of DC voltages. The Shapiro-Wilk test was

used to conduct statistical analysis on the breakdown voltages of punga oil and to ensure that breakdown voltage follows a normal distribution, the significance level of hypothesis was set at 95%, where the p-value is used to rank distributions and detect the likelihood of hypothesis. The null hypothesis is accepted if the p-value is greater than the significance level ($\alpha = 0.05$). The W Statistic, which is employed in the Shapiro-Wilk test [34], is calculated as follows:

$$W = \frac{(\sum_{i=1}^{n} a_i x_i)^2}{\sum_{i=1}^{n} (x_i - \bar{x})^2} \tag{3}$$

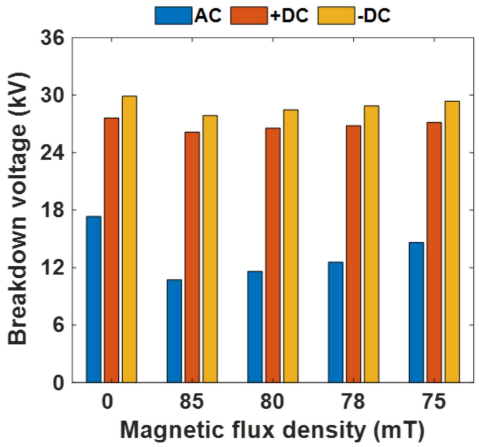

FIGURE 10. Breakdown of punga oil under different flux densities and voltage profiles.

The test statistic being calculated was compared to a pre-tabulated list based on the observation data and this comparison gave a higher p-value than the significance level. Similar results have been inferred in the previous works by the authors on the natural ester fluids [20] and thus, the null hypothesis test towards normal distribution was accepted towards the breakdown characteristics of punga oil. Still now, the breakdown voltage of ester fluid has been investigated without the effect of magnetic field and it was observed to follow a normal distribution with large deviations at the lower and upper percentiles [35]. In the present study, the breakdown voltage of punga oil with the effect of magnetic field is studied and the test accepts the null hypothesis of normal distribution, as shown in Table 6.

The Kolmogorov–Smirnovtest was also used to check for the extreme value distribution, which resulted in a lower p-value. The probability plot of breakdown voltage on punga oil under AC and DC voltages with the effect of magnetic field is shown in Fig. 11. There was not much scatter in the breakdown voltage except at lower and higher probability percentiles.

D. DIELECTRIC RESPONSE SPECTROSCOPY

The dielectric response studies were carried out with punga oil at different temperatures using OMICRON-DIRANA unit and the results are provided in Table 7 for measurements

TABLE 6. Hypothesis test of confirmity towards normal distribution under different voltage profiles and magnetic fields.

B_{max} (mT)	AC		+DC		–DC	
	Statistic (W)	p-value	Statistic (W)	p-value	Statistic (W)	p-value
0	0.9453	0.3019	0.9334	0.1794	0.9251	0.1247
85	0.9559	0.4599	0.9529	0.4138	0.9456	0.3053
80	0.9349	0.1923	0.9264	0.1319	0.9720	0.7978
78	0.9634	0.6147	0.9334	0.1795	0.9517	0.3931
75	0.9496	0.3624	0.9381	0.2209	0.9432	0.2750

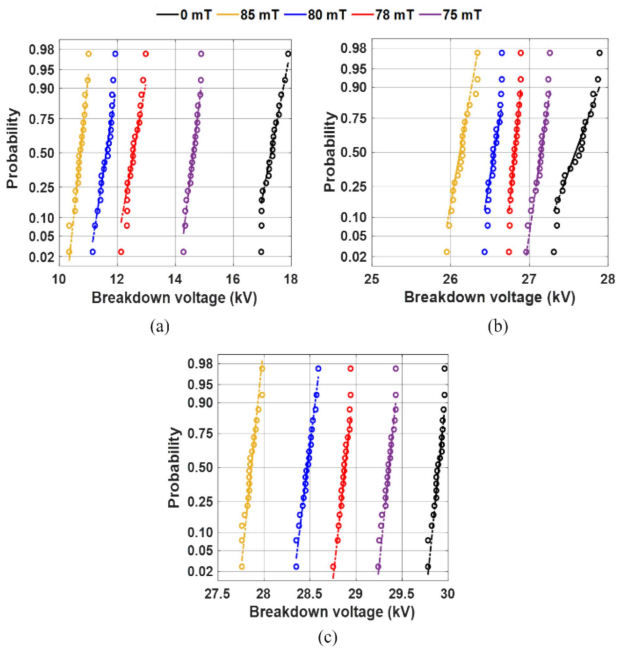

FIGURE 11. Normal probability of breakdown voltage on punga oil under (a) AC voltage, (b) +DC voltage, (c) –DC voltage.

performed at 50 Hz. It is observed that increase in the temperature has reduced the dielectric constant which could be due to the weaker contact force between molecules of the fluid as well as the reduction in its kinematic viscosity [36]. The ester fluid undergoes oxidative breakdown of unsaturated fatty acids at higher temperatures and the hydrogen atom's free radical reaction enhances conductivity in the oil matrix.

Table 7 also reveals a temperature-dependent rise in the loss tangent with an increase of about 338% observed at 90°C compared to ambient temperature (30°C), which could be attributed to larger relaxation loss at higher temperatures. It is observed that tan δ decreases with increase in the frequency (Fig. 12). The slow polarization and depolarization mechanism at lower frequencies [37] increases the dielectric losses with no significant variation its magnitude, whereas at higher frequencies a significant change is observed with a reduction in its tan δ values. The orientation of polar molecules formed

TABLE 7. Dielectric constant and dissipation factor at power frequency (50 Hz).

Temperature (°C)	ε_r	tan δ
30	3.28	1.7558
50	3.21	3.4531
70	2.98	5.7442
90	2.96	7.6911

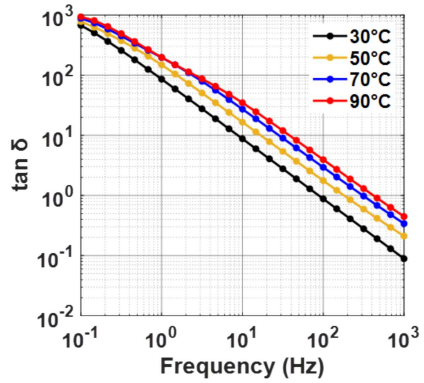

FIGURE 12. Variation in dissipation factor of punga oil with frequency at different temperatures.

in the ester fluid and hopping of charge carriers at higher temperatures results in the increase in the dielectric losses. Although the dissipation factor of punga oil is very high compared to conventional mineral oil, considering the literature available on punga oil for its other dielectric properties such as breakdown strength, permittivity and higher flash point [38], it is considered suitable for its application towards transformers after the transesterification process [6].

E. ELECTROSTATIC CHARGING TENDENCY (ECT) OF PUNGA OIL

The streaming current of punga oil measured with respect to different temperatures and disc velocity is shown in Table 8. It is observed that streaming current did not show much variation with disc velocity upto 300 rpm but at higher disc velocities (>300 rpm), a significant change in the current has been noticed. This sudden increase in the current could be associated with higher friction exerted between the fluid/pressboard [39]. With increase in the temperature, the rise in the current observed at 90°C is around six times higher than that measured at ambient temperature (30°C). The increase in the charge density and ionic mobility of fluid at higher temperatures could be responsible for the increase in the streaming current [40]. On comparing these results with the conventional mineral oil, the charging tendency of mineral oil is very low due to inherent aromatic suppressants [33]. Also, these higher charging current observed in punga oil could be reduced by adding optimum amount of benzotriazole (BTA) additive which has been illustrated in our previous studies [40]. Thus, the convection of charges around the electrical double layer of the fluid/pressboard interface elucidates the electrostatic charging tendency of punga oil.

TABLE 8. Streaming current of punga oil with disc velocity and temperature.

Disc velocity (rpm)	Streaming current (pA)			
	30°C	50°C	70°C	90°C
100	8.27	21.17	41.16	78.89
200	44.1	98.36	136.34	224.45
300	76.91	187.86	276.87	634.56
400	133.25	367.83	674.56	1154.56
500	182.54	598.86	945.67	1878.67
600	387.85	882.23	1234.45	2456.67

IV. CONCLUSION

In this work, we have reported the experimental investigation of the impact of magnetic field in the corona discharge activity of punga oil for different AC and DC voltage conditions using fluorescent fiber sensor as well as UHF sensor techniques. The salient findings of our work are as follows:

- Corona inception voltage (CIV) measured using both fluorescence sensor and UHF sensor showed a higher magnitude under DC voltages compared to AC voltage. From the sensitivity perspective, the white fluorescent fiber detected the discharges at an early stage followed by red fluorescent fiber and UHF sensor.
- The spectrum of the UHF signal obtained under AC voltage shifted towards lower frequency (0.6 GHz) under the influence of magnetic flux density of 85 mT. Although the presence of magnetic field did not affect the CIV of punga oil under DC voltages, the corresponding UHF signal has shifted towards higher frequency (1.35 GHz). On the other hand, the fluorescent fiber signal measured using white fiber or the red fiber did not show any variation in the spectrum for different flux densities.
- The rise time, pulse width and energy content of the fluorescent signal formed due to corona activity under AC voltage is found to be higher at flux density of 85 mT compared to a flux density less than 80 mT. Also, not much variation is observed with the fluorescent signal formed due to corona discharges under DC voltages, in presence of magnetic field.
- PRPD analysis clearly indicates that corona discharge occurred near the peak of the applied AC voltage and no change in the phase window is measured. Also, the phase at which discharge occurs is observed to be consistent with both fluorescent fiber sensor as well as UHF sensor.
- The breakdown voltage was higher under DC voltages compared to AC voltage with significant variation observed only at flux density greater than 80 mT. Also, the statistical analysis performed on the breakdown voltage of punga oil with the effect of magnetic field followed normal distribution which was confirmed through the hypothesis testing.

- The dielectric studies show that the permittivity of punga oil does not change significantly with temperature, whereas the dissipation factor increased dramatically to about 338% at higher temperatures compared to ambient temperature conditions.
- The streaming current of punga oil showed only a minimal change for different disc velocities and a marginal change was exhibited only at disc velocities greater than 300 rpm. At higher temperature (90°C), the charging current was around five times larger than that observed at ambient temperature.

REFERENCES

[1] X. Wang, C. Tang, B. Huang, J. Hao, and G. Chen, "Review of research progress on the electrical properties and modification of mineral insulating oils used in power transformers," *Energies*, vol. 11, no. 3, p. 487, Feb. 2018.

[2] R. Asano and S. A. Page, "Reducing environmental impact and improving safety and performance of power transformers with natural ester dielectric insulating fluids," *IEEE Trans. Ind. Appl.*, vol. 50, no. 1, pp. 134–141, Jan./Feb. 2014.

[3] Z. Shen, F. Wang, Z. Wang, and J. Li, "A critical review of plant-based insulating fluids for transformer: 30-year development," *Renew. Sustain. Energy Rev.*, vol. 141, May 2021, Art. no. 110783.

[4] D. M. Mehta, P. Kundu, A. Chowdhury, V. K. Lakhiani, and A. S. Jhala, "A review on critical evaluation of natural ester vis-a-vis mineral oil insulating liquid for use in transformers: Part 1," *IEEE Trans. Dielectr. Electr. Insul.*, vol. 23, no. 2, pp. 873–880, Apr. 2016.

[5] S. A. Ghani, N. A. Muhamad, Z. A. Noorden, H. Zainuddin, N. A. Bakar, and M. A. Talib, "Methods for improving the workability of natural ester insulating oils in power transformer applications: A review," *Electr. Pow. Syst. Res.*, vol. 163, pp. 655–667, Oct. 2018.

[6] N. Baruah, M. Maharana, and S. K. Nayak, "Performance analysis of vegetable oil-based nanofluids used in transformers," *IET Sci., Meas. Technol.*, vol. 13, no. 7, pp. 995–1002, Sep. 2019.

[7] S. Mitra, A. Ghose, N. Gujre, S. Senthilkumar, P. Borah, A. Paul, and L. Rangan, "A review on environmental and socioeconomic perspectives of three promising biofuel plants *Jatropha curcas, pongamia pinnata and Mesua ferrea*," *Biomass Bioenergy*, vol. 151, Aug. 2021, Art. no. 106173.

[8] T. Mariprasath, V. Kirubakaran, S. Madichetty, and K. Amaresh, "An experimental study on spectroscopic analysis of alternating liquid dielectrics for transformer," *Electr. Eng.*, vol. 103, no. 2, pp. 921–929, Apr. 2021.

[9] R. Thanigaiselvan, T. S. R. Raja, and R. Karthik, "Investigations on eco friendly insulating fluids from rapeseed and pongamia pinnata oils for power transformer applications," *J. Electr. Eng. Technol.*, vol. 10, no. 6, pp. 2348–2355, Nov. 2015.

[10] C. Rakesh and M. J. Thomas, "Pongamia oil, an eco-friendly alternative for mineral oil used in high voltage transformers," in *Proc. IEEE Int. Conf. Dielectr. (ICD)*, Jul. 2016, pp. 959–962.

[11] C. G. Azcarraga, A. Cavallini, and U. Piovan, "A comparison of the voltage withstand properties of ester and mineral oils," *IEEE Elect. Insul. Mag.*, vol. 30, no. 5, pp. 6–14, Sep. 2014.

[12] M. R. Hussain, S. S. Refaat, and H. Abu-Rub, "Overview and partial discharge analysis of power transformers: A literature review," *IEEE Access*, vol. 9, pp. 64587–64605, 2021.

[13] M. D. Judd, Y. Li, and I. B. B. Hunter, "Partial discharge monitoring of power transformers using UHF sensors. Part I: Sensors and signal interpretation," *IEEE Elect. Insul. Mag.*, vol. 21, no. 2, pp. 5–14, Mar./Apr. 2005.

[14] H. Chai, B. T. Phung, and S. Mitchell, "Application of UHF sensors in power system equipment for partial discharge detection: A review," *Sensors*, vol. 19, no. 5, p. 1029, Feb. 2019.

[15] J. M. Martínez-Tarifa, J. Rivas-Conde, G. Robles, and J. Sanz-Feito, "Influence of leakage magnetic fields on partial discharge activity in power transformers," *IEEE Trans. Dielectr. Electr. Insul.*, vol. 17, no. 6, pp. 1724–1730, Dec. 2010.

[16] S. K. Panigrahi, S. Thakur, R. Sarathi, and A. K. Mishra, "Understanding the physico-chemical properties of thermally aged natural ester oil adopting fluorescent technique," *IEEE Trans. Dielectr. Electr. Insul.*, vol. 24, no. 6, pp. 3460–3470, Dec. 2017.

[17] M. EL-Adawy, T. Paillat, G. Touchard, and J. Cabaleiro, "Numerical simulation of the electrical double layer development: Physicochemical model at the solid and dielectric liquid interface for laminar flow electrification phenomenon," *IEEE Trans. Dielectr. Electr. Insul.*, vol. 18, no. 5, pp. 1463–1475, Oct. 2011.

[18] M. Zdanowski, "Streaming electrification phenomenon of electrical insulating oils for power transformers," *Energies*, vol. 13, no. 12, p. 3225, Jun. 2020.

[19] *Experience in Service With New Insulating Fluids*, document CIGRE Brochure 436, 2010.

[20] A. J. Amalanathan, R. Sarathi, S. Prakash, A. K. Mishra, R. Gautam, and R. Vinu, "Investigation on thermally aged natural ester oil for real-time monitoring and analysis of transformer insulation," *High Voltage*, vol. 5, no. 2, pp. 209–217, Apr. 2020.

[21] J. Tang, J. Zhou, X. Zhang, and F. Liu, "A transformer partial discharge measurement system based on fluorescent fiber," *Energies*, vol. 5, no. 5, pp. 1490–1502, May 2012.

[22] G. D. P. Mahidhar, R. Sarathi, and B. Srinivasan, "Fluorescence fiber based identification of partial discharges in liquid nitrogen for high-temperature superconducting power apparatus," *IEEE Sensors Lett.*, vol. 4, no. 2, pp. 1–4, Feb. 2020.

[23] *Insulating Liquids—Measurement of Relative Permittivity, Dielectric Dissipation Factor (Tan D) and D.C. Resistivity*, document IEC 60247, 2004.

[24] *Power Transformers—Part 2: Temperature Rise for Liquid-Immersed Transformers*, document IEC 60076-2, 2011.

[25] *Static Electrification in Power Transformers*, Cjw Communications Group, CIGRE, General Session, Paris, France, 2000.

[26] S. K. Panigrahi and A. K. Mishra, "Inner filter effect mediated red-shift in synchronous and total synchronous fluorescence spectra as a tool to monitor quality of oils and petrochemicals," *Fuel*, vol. 267, May 2020, Art. no. 117174.

[27] *Plastic Scintillating Fibers*. Accessed: Jul. 1, 2020. [Online]. Available: http://kuraraypsf.jp/psf/ws.html

[28] W. Worstell, S. Doulas, O. Johnson, and C.-J. Lin, "Scintillator crystal readout with wavelength-shifting optical fibers," in *Proc. IEEE Nucl. Sci. Symp. (NSS)*, Oct. 1994, pp. 1869–1873.

[29] R. Mangeret, J. Farenc, B. Ai, P. Destruel, D. Puretolas, and J. Casanovas, "Optical detection of partial discharges using fluorescent fiber," *IEEE Trans. Electr. Insul.*, vol. 26, no. 4, pp. 783–789, Aug. 1991.

[30] M. S. Godinho, M. R. Blanco, F. F. G. Neto, L. M. Lião, M. M. Sena, R. Tauler, and A. E. de Oliveira, "Evaluation of transformer insulating oil quality using NIR, fluorescence, and NMR spectroscopic data fusion," *Talanta*, vol. 129, pp. 143–149, Nov. 2014.

[31] D. Siebler, P. Rohwetter, R. Brusenbach, and R. Plath, "Optical-only detection of partial discharge with fluorescent polymer optical fiber sensors," *Proc. Eng.*, vol. 120, pp. 845–848, Jan. 2015.

[32] A. J. Reid, M. D. Judd, R. A. Fouracre, B. G. Stewart, and D. M. Hepburn, "Identification of simultaneously active partial discharge sources using combined radio frequency and IEC60270 measurement," *IET Sci., Meas. Technol.*, vol. 5, no. 3, pp. 102–108, May 2011.

[33] J. Xiang, Q. Liu, and Z. D. Wang, "Inception and breakdown voltages of insulating liquids under DC stress," in *Proc. IEEE Int. Conf. High Voltage Eng. Appl. (ICHVE)*, Sep. 2016, pp. 1–4.

[34] A. Beroual, U. Khaled, P. M. Noah, and H. Sitorus, "Comparative study of breakdown voltage of mineral, synthetic and natural oils and based mineral oil mixtures under AC and DC voltages," *Energies*, vol. 10, no. 4, p. 511, 2017.

[35] Y. Jing, I. V. Timoshkin, M. P. Wilson, M. J. Given, S. J. MacGregor, T. Wang, and J. M. Lehr, "Dielectric properties of natural ester, synthetic ester midel 7131 and mineral oil Diala D," *IEEE Trans. Dielectr. Electr. Insul.*, vol. 21, no. 2, pp. 644–652, Apr. 2014.

[36] M. H. A. Hamid, M. T. Ishak, M. F. M. Din, N. S. Suhaimi, and N. I. A. Katim, "Dielectric properties of natural ester oils used for transformer application under temperature variation," in *Proc. IEEE Int. Conf. Power Energy (PECon)*, Nov. 2016, pp. 54–57.

[37] S. Thakur, R. Sarathi, and M. G. Danikas, "Investigation on thermal ageing impact on dielectric properties of natural ester oil," *Electr. Eng.*, vol. 101, no. 3, pp. 1007–1018, Sep. 2019.

[38] T. Mariprasathn and V. Kirubakaran, "A critical review on the characteristics of alternating liquid dielectrics and feasibility study on pongamia pinnata oil as liquid dielectrics," *Renew. Sustain. Energy Rev.*, vol. 65, pp. 784–799, Nov. 2016.

[39] I. Kolcunová, J. Kurimský, R. Cimbala, J. Petráš, B. Dolník, J. Džmura, and J. Balogh, "Contribution to static electrification of mineral oils and natural esters," *J. Electrostatics*, vol. 88, pp. 60–64, Aug. 2017.
[40] A. J. Amalanathan, R. Sarathi, N. Harid, and H. Griffiths, "Investigation on flow electrification of ester-based TiO_2 nanofluids," *IEEE Trans. Dielectr. Electr. Insul.*, vol. 27, no. 5, pp. 1492–1500, Oct. 2020.

SRINIVASAN MURUGESAN (Member, IEEE) was born in Tamil Nadu, India, in 1987. He received the B.E. degree in electrical engineering from Erode Sengunthar Engineering College, Erode, Tamil Nadu, the M.E. degree in high voltage engineering from the National Engineering College, Kovilpatti, Tamil Nadu, and the Ph.D. degree from Anna University, Chennai. He is currently working as an Assistant Professor with Kongu Engineering College, Perundurai, Tamil Nadu. His research interests include alternative insulating fluids, eco-friendly fire-resistant fluids, insulation engineering, and power systems.

A. J. AMALANATHAN is currently a Research Scholar with the Department of Electrical Engineering, IIT Madras, Chennai, India. His research interest includes condition monitoring of ester and its nano-fluids for power transformers.

R. SARATHI (Senior Member, IEEE) is currently a Professor and the Head of the High Voltage Laboratory, Department of Electrical Engineering, IIT Madras, Chennai, India. His research interest includes condition monitoring of power apparatus and nanomaterials.

BALAJI SRINIVASAN (Member, IEEE) is currently a Professor with the Department of Electrical Engineering, IIT Madras, Chennai, India. His research interests include development of active and passive optical components/subsystems for distributed fiber optic sensors and fiber lasers.

RAVI SAMIKANNU (Senior Member, IEEE) received the Ph.D. degree in electrical engineering from Anna University, Chennai, India. He is currently working as an Associate Professor with the Electrical, Computer, and Telecommunications Engineering Department, Botswana International University of Science and Technology (BIUST), Palapye, Botswana. He is working on research projects in power system, energy systems, and smart grid.